Geophys. J. Int. (1995) 123, 611-622

Age models, sediment fluxes and palaeoclimatic reconstructions for the Chinese loess and palaeosol sequences

R. Thompson[1] and B. A. Maher[2]
[1]*Department of Geology and Geophysics, Grant Institute, University of Edinburgh, West Mains Road, Edinburgh* EH9 3JW, *UK*
[2]*School of Environmental Sciences, University of East Anglia, Norwich* NR4 7TJ, *UK*

Accepted 1995 June 14. Received 1995 May 17; in original form 1995 January 27.

SUMMARY

Palaeomagnetic studies of the Chinese loess provided the first firm chronology for these sediments and revealed that their depositional history reaches back over 2.5 Ma. Magnetic susceptibility records can provide an even more detailed chronology through correlation with the $\ddot{e}^{18}O$ deep-sea stratigraphy. The susceptibility fluctuations have been used also, either alone or in combination with ^{10}Be measurements, to reconstruct palaeoclimate. However, there is still debate as to the origin of the ^{10}Be and magnetic minerals in the Chinese loess and hence their palaeoclimatic significance. Here we analyse magnetic data from six sites across the Loess Plateau, and reinterpret the ^{10}Be data from Luochuan as largely reflecting primary ^{10}Be dust loading rather than as a palaeorainfall indicator. We discount previous ideas of both constancy of the flux of magnetically susceptible minerals (i.e. susceptibility flux) or constancy of the ratio of the flux of ^{10}Be and susceptibility. We explain the susceptibility of Chinese loess in terms of *in situ* pedogenic ferrimagnetic enhancement. The competing effects of reduction and oxidation are taken to control the degree of magnetic enhancement, such that magnetic susceptibility is a direct indicator of palaeorainfall. Our reconstructions yield variations in palaeorainfall of between +28 per cent and —12 per cent in the central Loess Plateau rather than +100 per cent to —50 per cent as suggested from previous ^{10}Be and magnetic susceptibility studies.

Key words: ^{10}Be, China, loess, magnetic susceptibility, palaeoclimate, palaeorainfall.

1 INTRODUCTION

Nowhere in the terrestrial environment is there a more complete and highly resolved archive of Quaternary climate change than in the Loess Plateau region of north central China. Deposition of windblown dust in this area (between latitudes 33° and 47°N, longitudes 127° and 75°E, Fig. la) was initiated around 2.5 Ma BP (Heller & Liu 1986). A vast volume of sediment, provided from sources such as the Gobi Desert and the Tibetan Plateau, completely buries the previous surface topography. The volume of dust on the Loess Plateau and its margins (0.5×10^3 km^3) can be approximately related to the volume of, for example, the mountains of Scandinavia. Loess transport and deposition were at a maximum during cool, dry (glacial) stages. During warmer, wetter (interglacial/interstadial) stages, vegetation more permanently colonized the loess surface and *in situ* weathering enhanced development of soil horizons. Cyclical variations in climate produced multiple interleaving of less-weathered loess layers with reddened, clay-enriched palaeosols.

In a spatial sense, the loess/palaeosol sequences are a wedge, up to 350 m thick in the western Plateau (e.g. around Lanzhou), about 150 m thick in the central area (e.g. Luochuan), thinning out further to the south and east. The sediments are also finer grained from west to south and east. These variations span a contemporary climatic gradient (Fig. lb), from relatively dry in the west (≈350 mm rainfall yr^{-1}) to increasingly humid in the south and east (≈700 mm yr^{-1}).

Only qualitative assessment of changes in palaeoclimate can be made from the lithostratigraphic variations of the loess/soil sequences. The loess/soil fossil record (of pollen and snails) also lacks resolution, owing to poor preservation and problems in classification. However, quantitative palaeoclimatic reconstructions have recently been attempted for these sediments by analysis of their rock magnetic properties (Maher, Thompson & Zhou 1994) and their content of beryllium-10, a cosmogenic radionuclide (Heller *et al.* 1993). Both sets of these measured properties show strong correlation with each other and with the deep-sea $S^{18}O$ record, indicating that they are both responding to climate change in some, not necessarily linked, way. In terms of the rock magnetic properties, magnetic susceptibility values, for instance, are higher by a factor of

© 1995 RAS

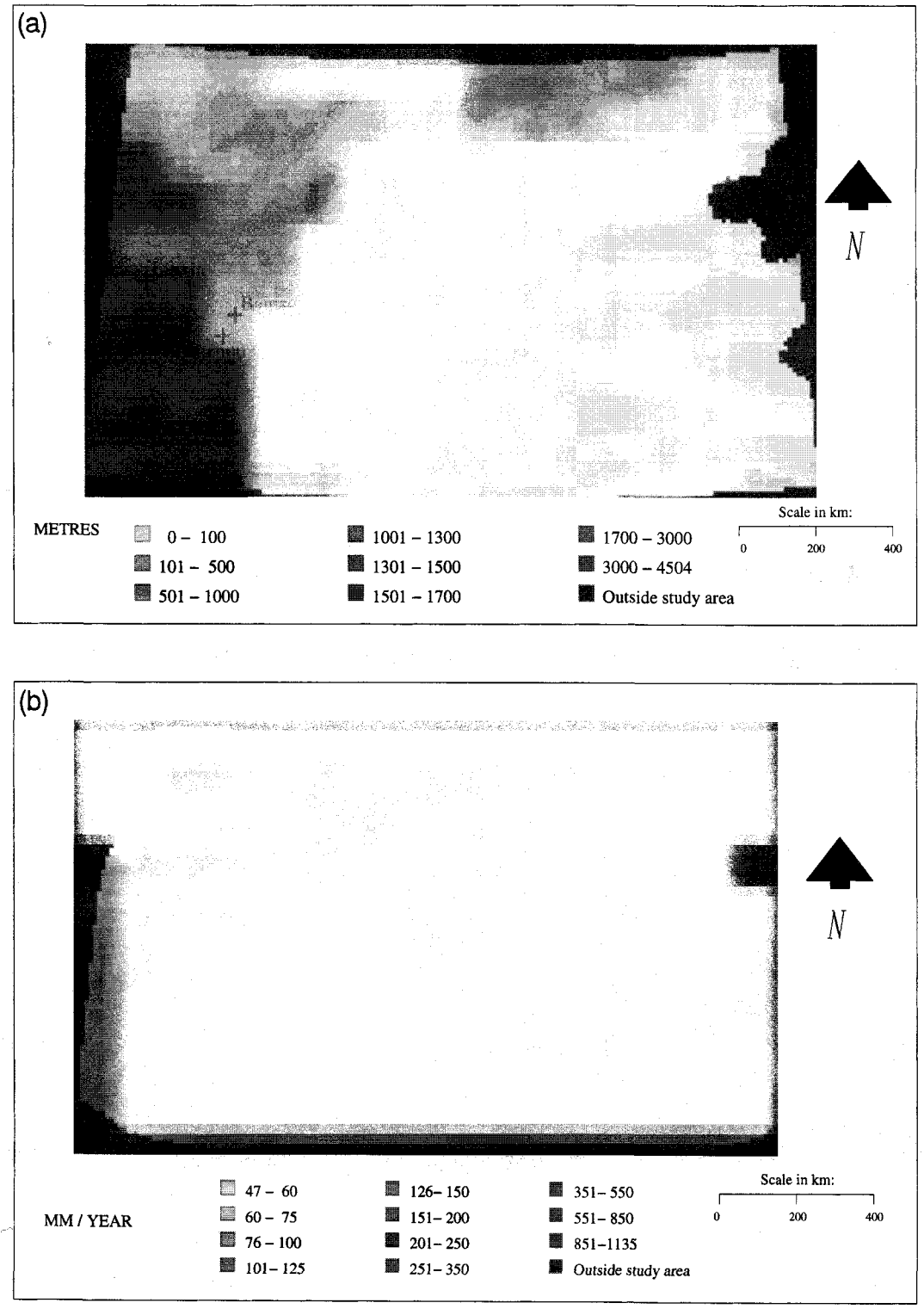

Figure 1. The Chinese Loess Plateau and its surroundings: (a) topography; (b) annual precipitation.

between three and six in the palaeosols than in the intervening loess layers. Similarly, ^{10}Be concentrations are also higher in the palaeosols, but by a smaller factor, between two and three.

In the case of the ^{10}Be studies, a ^{10}Be record was obtained for the loess/soil sequence at Luochuan, in the central part of the Loess Plateau (Shen *et al.* 1992). The fluxes of ^{10}Be and magnetic susceptibility were calculated, and the ^{10}Be flux owing to detrital input used to identify the detrital and the *in situ* (pedogenic) components of susceptibility. The pedogenic component, related directly to regional rainfall, was then used to reconstruct palaeorainfall for the last glacial/interglacial cycle (Heller *et al.* 1993).

In the approach of Maher *et al.* (1994), magnetic susceptibility alone was used to reconstruct palaeorainfall, for a range of

sites across the Loess Plateau. Absolute values of pedogenic susceptibility were used, rather than calculated fluxes of susceptibility. The relationship between pedogenic susceptibility and rainfall was calibrated by susceptibility measurements of modern soils in the Loess Plateau region. Table 1 summarizes the two sets of rainfall reconstructions resulting from these two approaches.

Here, we try to account for the obvious differences between the two sets of rainfall reconstructions, by exploring (a) the differences between the two approaches, (b) the physical processes involved in the climatic responses of the two sets of proxy indicators (^{10}Be and pedogenic magnetic susceptibility), and (c) problems in data analysis, particularly with regard to the calculation of sediment accumulation rates and ^{10}Be/susceptibility fluxes.

2 DATING OF THE CHINESE LOESS AND FLUX CALCULATIONS

Much of the early work done on the Chinese Loess Plateau was aimed at establishing lithostratigraphic correlation across the region. However, increasing attention is being paid to identifying an absolute chronostratigraphy for the sequences (Table 2). Here, we first compare the dating results obtained for sites across the Loess Plateau from various dating models and techniques, and then consider the implications of these results for calculations of accumulation rates and fluxes. Fig. 2 shows dating results and rock magnetic data for a site in the western part of the Loess Plateau. The loess/soil sequence, close to the town of Linxia (33.5°N 103.1°E), is 40 m thick and rests unconformably upon an elevated river terrace. Samples were taken from the sequence at 10 cm and 20 cm intervals and subjected to rock magnetic analysis and dating by thermoluminescence (TL). The TL methods and data are described in detail by Zhou (in preparation). Also shown, in Fig. 2(a), is the δ^{18}O curve for deep-sea cores. Preliminary observation of the δ^{18}O data of Fig. 2(a) and the susceptibility data of Fig. 2(b) suggests that a strong match exists between the susceptibility and marine δ^{18}O records, and that the Linxia sequence represents a particularly highly resolved record of climate change over the last glacial/interglacial cycle. Individual climate substages appear well defined by the susceptibility record, as shown, for example, by the three separate peaks correlating with oxygen isotope stages 5a, c and e.

If we compare the TL-derived chronology with that obtained by correlating susceptibility with the dated δ^{18}O record, there is a general agreement between them, although the TL dates are systematically slightly younger. (Underestimation of the equivalent dose and also time-dependent signal loss have been reported as significant factors in dating loess by TL,

Table 1. Comparison of two sets of rainfall reconstructions for the last glacial–interglacial cycle, at Luochuan, Central Loess Plateau (35.7°N 109.4°E).

Present day rainfall : ~600 mm a^{-1}

Age		Correlated to δ^{18}O stage	Loess stratigraphy	Heller et al., 1993	Maher, Thompson & Zhou, 1994
Holocene	0 - 11 ka	1	S_0	No difference	See below
Early Holocene	~5 - 11 ka	1	S_0	See above	+ 23%
Last glacial	11 - 25 ka	2	L_1	- 50%	- 12%
	~ 25 ka	3	L_1SS_1	+ 100%	- 5%
	~ 55 ka	3	L_1SS_1	+ 100%	- 5%
	~55 - 70 ka	4	L_1	- 50%	- 12%
Last interglacial	~ 130 ka	5	S_1	- 14%	+ 28%

Table 2. Dating techniques and models applied to Chinese loess–palaeosol sequences.

Technique	Timescales (yr)	References
Palaeomagnetism: Events, reversals	10^3 - 10^6	Heller & Liu, 1982 Zheng et al., 1992 Zhu et al., 1994
Thermoluminescence	10^3 - 10^6	Zhou et al., 1992 Zhou (in prep)
Radiocarbon	10^2 - 40.10^3	Zhou et al., 1992
Uranium series (α-spectrometry)	~2.10^3 - 350.10^3	Rowe & Maher (in prep)
Magnetic susceptibility age models:		
(a) Constant flux model	10^4 - 10^6	Kukla et al., 1988
(b) Susceptibility matched to marine Minerogenic Accumulation Rate and thence matched to δ^{18}O record	5.10^3 - 5.10^5	Clemens & Prell, 1990 Hovan et al., 1989
(c) Susceptibility matched to δ^{18}O record	5.10^3 - 5.10^5	Maher & Thompson, 1992
Beryllium-10 age models:		
^{10}Be matched to δ^{18}O	5.10^3 - 5.10^5	Shen et al., 1992

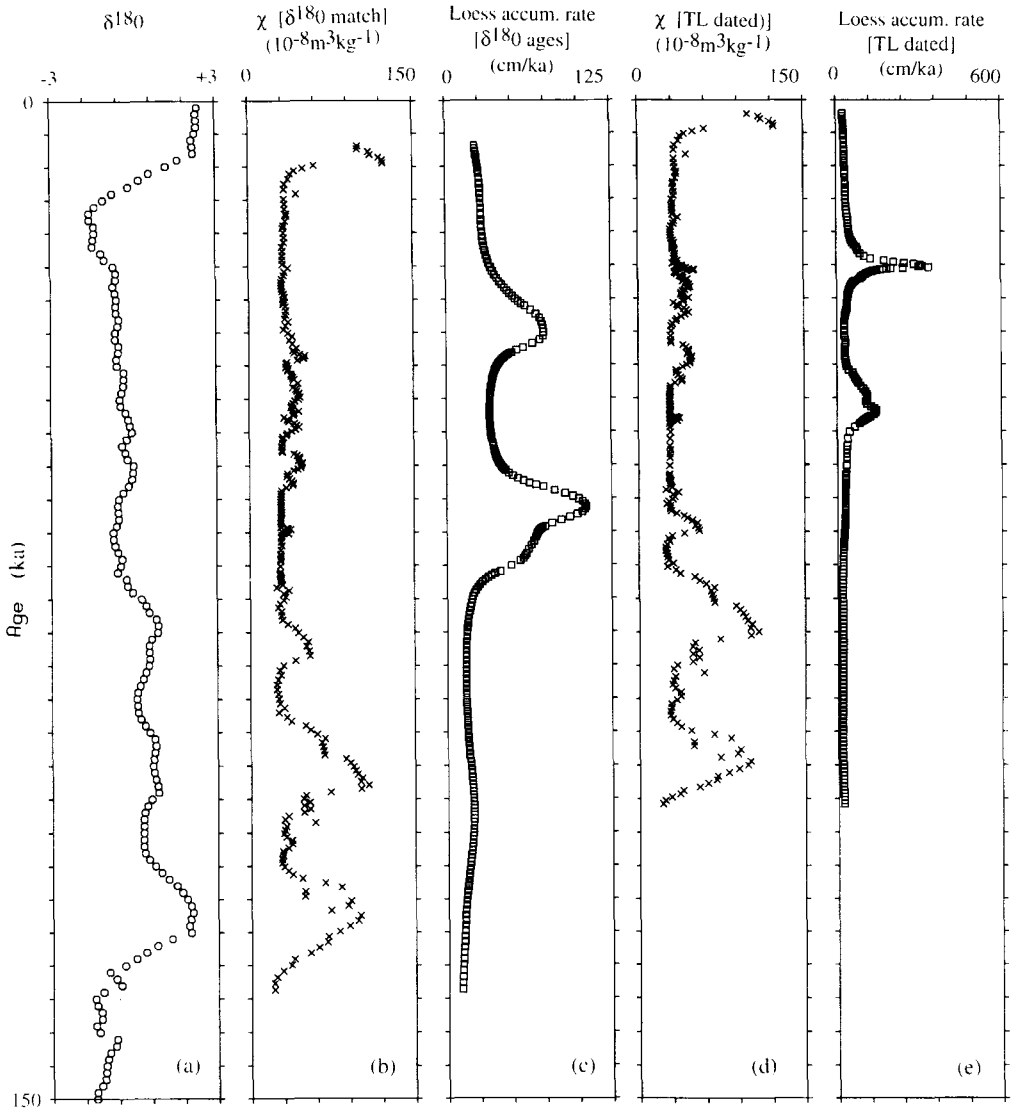

Figure 2. Loess accumulation rates at Linxia: (a) $\delta^{18}O$ chronology; (b) magnetic susceptibility (χ) matched to the $\delta^{18}O$ chronology; (c) loess accumulation rate based on the χ versus $\delta^{18}O$ matching of (b); (d) magnetic susceptibility dated by TL; (e) loess accumulation rate based on the TL ages of (d).

e.g. Rendell & Townsend 1988; Wintle 1990.) The differences between the two age models become obvious and particularly important when accumulation rates and fluxes are subsequently calculated from them (Figs 2c and e). The compressed chronology of the TL data produces a marked spike in the calculated loess accumulation rate at $\approx$26 ka and a broader peak at $\approx$50 ka (Fig. 2e). The $\delta^{18}O$/susceptibility match results in much broader peaks in accumulation rate between $\approx$25–40 ka and 55–75 ka (Fig. 2c). Hence, as in all studies involving calculation of sediment accumulation rates and mineral fluxes, such calculations depend crucially on the age model used and its accuracy.

Notwithstanding this caveat regarding flux calculations, if we extend our comparison of age models and flux calculations to other dated sequences in the region and its offshore margin, the spatial pattern of sediment and susceptibility flux can be examined. Fig. 3 summarizes the susceptibility–depth data and Table 3 tabulates the susceptibility fluxes obtained for (from west to east and south) Linxia (35.3°N 103.1°E), Xifeng (35.7°N 107.6°E) Luochuan (35.6°N 109.3°E), Quinjiazhi (35.7°N 109.8°E), Baoji (34.2°N 107.1°E) and West Pacific core V-21-146. The dating approaches (Table 2) for these sequences encompass absolute dating methods (e.g. TL, radiocarbon, uranium-series), and age-modelling by correlation (e.g. $\delta^{18}O$ matched with ^{10}Be at Luochuan; Shen *et al.* 1992). Overall, there is again good general agreement between the various age estimates, within about 10 ka, for a range of sites across the region. However, in contrast with the absolute dating methods, many of the age-model approaches involve the use of calculated fluxes. Kukla *et al.*'s (1988) dating method, for instance, depends entirely on the assumption of a constant calculated value of susceptibility flux. Hovan *et al.* (1989) matched their calculated minerogenic accumulation rates (MAR) in West Pacific cores to susceptibility in the Chinese loess. Similarly, Clemens & Prell (1990) matched MAR in Indian Ocean cores to the loess susceptibility record. The use of calculated accumulation rates and fluxes has important ramifications both for the chronological models thus derived and for subsequent

© 1995 RAS, *GJI* 123, 611–622

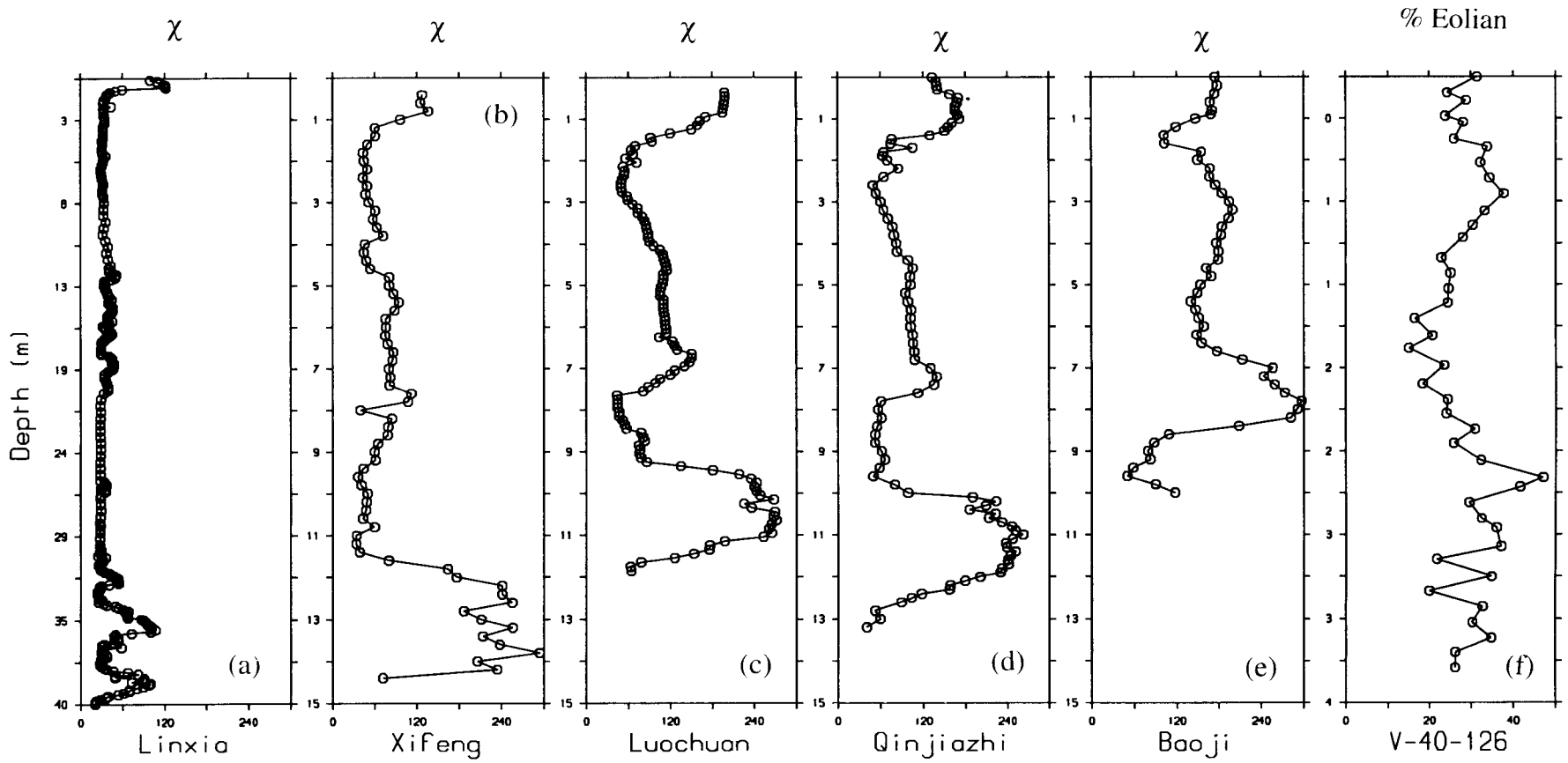

Figure 3. Magnetic susceptibility concentration along a W–E transect through the last interglacial–glacial–interglacial cycle at five sites (a) to (e) and eolian concentration at one site (f) in the Northern Pacific. Note that the extreme western (a) and eastern (f) localities have different depth scales. The magnetic susceptibility accumulation rates in Table 3, which shows very variable magnetic susceptibility accumulation rates both within and between sites, are calculated from the data shown here.

Table 3. Magnetic susceptibility accumulation rates from west to east across the Chinese loess deposits.

Duration	Unit	Linxia	Xifeng	Luochuan	Quinjiazhi	Baoji	V-40-126
(ka)		(Susceptibility accumulation rate+ in units of 10^{-8} m^4 kg^{-1} ka^{-1})					
11	S_0	5	6	16	18	15	---
60	L_1	24	12	10	11	13	5.2
58	S_1	4	8	5	6	5	2.4

+ Susceptibility accumulation rate (m^4 kg^{-1} ka^{-1}) = Loess accumulation rate (m ka^{-1}) * Volume susceptibility (dimensionless) / density (kg m^{-3})

interpretation of the loess climate proxies, susceptibility and ^{10}Be, as discussed below.

A notable feature of the data shown in Fig. 3 is the demonstration that susceptibility flux is *not* constant across the Loess Plateau area. Rather, flux values vary significantly from west to east (Table 3). For palaeosol S_0, susceptibility flux tends to increase from west to south and east. Flux values for L_1 (including the Stage 3 interstadial soil) are particularly high in the west ($>20\times10^{-8}$ m^4 kg^{-1} ka^{-1}) owing to the combination of high sediment accumulation rates and moderate susceptibility values. The L_1 susceptibility flux falls off steadily to the east. S_1 susceptibility fluxes are particularly low right across the Loess Plateau and then decrease further in the Pacific. Even in the central part of the Loess Plateau, where susceptibility flux has varied the least, we find variations of a factor of two to three in the most recent interglacial–glacial–interglacial period. We find no evidence for constancy of susceptibility flux during the last million years.

Fig. 4 illustrates a further approach to dating of the Chinese loess. Shen *et al.* (1992), Beer *et al.* (1993) and Heller *et al.* (1993) prefer to match ^{10}Be concentration to δ^{18}O. Sequence slotting (Thompson & Clark 1993) of δ^{18}O (Fig. 4a) and ^{10}Be (Fig. 4b) results in the loess accumulation rates of Fig. 4(c) and the ^{10}Be accumulation rates of Fig. 4(d). Notice how the ^{10}Be accumulation rates are much more dependent on the loess accumulation rates than on the ^{10}Be concentrations and once again how critical the age model is in any palaeoclimatic reconstruction based on accumulation rates or fluxes.

3 PALAEOCLIMATE

3.1 Rainfall reconstructions

We consider three quantitative approaches to rainfall reconstruction. These involve:

(1) magnetic susceptibility alone,
(2) beryllium-10 alone, and
(3) a paired magnetic susceptibility/beryllium-10 approach.

For each approach, it is necessary to assess the effects on the rainfall calculations of (1) the original loess-dust input (2) the loess accumulation rate and (3) the post-depositional processes and their dependence on rainfall.

3.1.1 Method 1: magnetic susceptibility

Maher *et al.* (1994) have proposed that magnetic susceptibility can be used as an independent measure of rainfall in the Chinese Loess Plateau region through use of the equation:

$$\underset{(\mathrm{mm\ yr^{-1}})}{\mathrm{Rain}} = 222 + 199 \log 10\,(\underset{(10^{-8}\ \mathrm{m^3\ kg^{-1}})}{\chi_B} - \chi_C), \quad (1)$$

where χ_B is the peak magnetic susceptibility of the sampled layer and χ_C is the magnetic susceptibility of the original loess-dust at the time of deposition. The difference $\chi_B-\chi_C$ is the magnetic susceptibility produced at the site by post-depositional pedogenic processes. Eq. (1) was constructed by a least-squares regression analysis of the susceptibility of modern-day calibration soils collected from different climatic areas within the Loess Plateau.

The two key assumptions associated with the use of eq. (1) are that (**a**) the magnetic susceptibility of the loess-dust deposited at any site varies little with time and consequently can be approximated by the minimum value at the site e.g. $\chi_C \approx \chi_{L9} (\approx 20\times10^{-8}$ m^3 $kg^{-1})$ and (**b**) pedogenic magnetic susceptibility in Chinese loess soils enhances towards a peak, steady-state value in around 5×10^3 years or less.

Susceptibility is very easy to measure and so this first approach to rainfall reconstruction can be applied to high-resolution studies from many stratigraphic sequences across the Loess Plateau. It is worth emphasizing that, because magnetic susceptibility is assumed to enhance rapidly towards a peak, steady-state value, accumulation rates do not influence the rainfall reconstructions. In essence, in Method 1, high susceptibility (high magnetite concentration) corresponds to high palaeorainfall, and low susceptibility (low magnetite concentration) to low palaeorainfall.

Table 4 summarizes the results from the application of Method 1 to the five Loess Plateau sites of Fig. 3, for the last glacial/interglacial cycle. We find higher average rainfall for the early to mid Holocene than at the present day. Reduced rainfall is found for glacial times, particularly in the east and south. The highest palaeorainfalls are found for the last interglacial.

3.1.2 Method 2: beryllium-10

Before discussing a joint magnetic-susceptibility/^{10}Be approach to palaeorainfall reconstruction, it is instructive to consider a

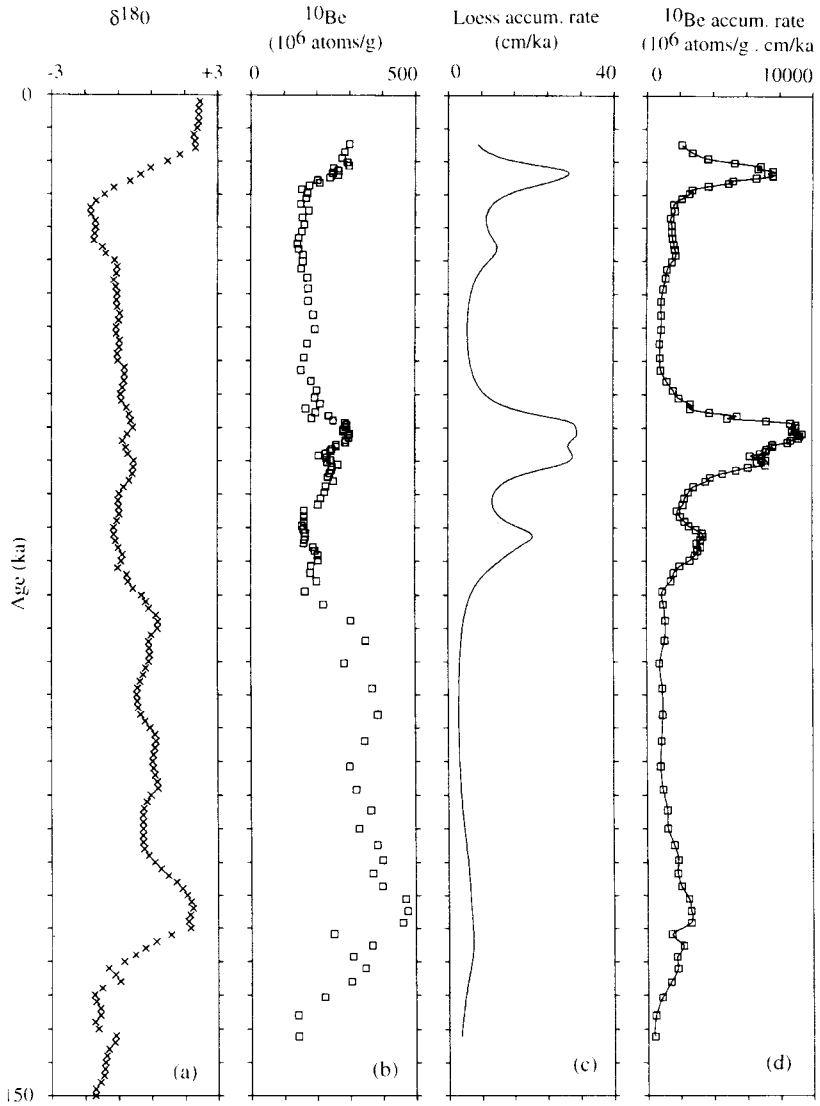

Figure 4. Luochuan: ^{10}Be concentration, accumulation rate and flux. (a) δ^{18}O chronology; (b) ^{10}Be concentration matched to the δ^{18}O chronology; (c) loess accumulation rate based on the match of (a) and (b); (d) ^{10}Be accumulation rate. Note how the ^{10}Be accumulation rate mainly reflects the loess accumulation rate of (c) and not the ^{10}Be concentration of (b).

method based on ^{10}Be alone. In principle, ^{10}Be in loess could be used to estimate palaeorainfall as long as certain simplifying assumptions hold. Pavich *et al.* (1986) describe how the ^{10}Be inventory of soils mainly depends on the duration of their exposure to rainfall. Following its production in the upper atmosphere, ^{10}Be is rapidly scavenged by raindrops and transported to the Earth's surface where it is strongly adsorbed onto clay minerals. Owing to the high retention of ^{10}Be by clays, old soils have high ^{10}Be concentrations. In their study of Californian soils, Pavich *et al.* (1986) point out that in the

Table 4. Palaeorainfall reconstructions from west to east across the Chinese Loess Plateau.

Duration	Unit	Linxia	Xifeng	Luochuan	Quinjiazhi	Baoji	
1950 - 1990 AD		431	522	537	537	565	Rainfall in mm a^{-1}
11 ka	S_0	+44	+23	+23	+20	+13	Percentage change
60 ka	L_1	-04	-10	-36	-22	-01	Percentage change
58 ka	S_1	+41	+32	+29	+27	+23	Percentage change
		35.5	35.7	35.7	35.7	34.3	Latitude (°N)
		103.1	107.6	109.4	109.8	107.2	Longitude (°E)

absence of soil erosion, or major changes in rainfall, ^{10}Be is a potential soil chronometer. Conversely, we note that if the exposure age of a soil were known, ^{10}Be would be a potential proxy of rainfall. To apply ^{10}Be to rainfall reconstruction from the loess record, it would first be necessary to separate the component of ^{10}Be brought on the original loess-dust from that component added later by rainfall. Following the subscript notation of Beer *et al.* (1993), we have

$$\underset{\text{(atoms)}}{I_B} = \underset{\text{(atoms)}}{I_A} + \underset{\text{(atoms)}}{I_D}, \quad (2)$$

where I_B is the total ^{10}Be influx, I_A is an atmospheric component, and I_D is the ^{10}Be influx associated with the loess-dust. Now

$$\underset{\text{(atoms)}}{I_D} = \underset{\text{(atoms g}^{-1})}{C_D} \times \underset{\text{(cm yr}^{-1})}{\delta Z/\delta T} \times \underset{\text{(g cm}^{-3})}{\sigma} \times \underset{\text{(yr)}}{t} \quad (3)$$

and

$$\underset{\text{(atoms)}}{I_A} = \underset{\text{(atoms yr}^{-1})}{R} \times \underset{\text{(yr)}}{t}, \quad (4)$$

where C_D is the concentration of ^{10}Be on the loess-dust at the time of deposition, $\delta Z/\delta t$ is the accumulation rate, σ is the density, t is the period of accumulation, and R is the loading of ^{10}Be from rainfall.

If we could assume that (c) C_D has remained roughly constant over time (e.g. $C_D \approx C_{L9}$) and that (d) the concentration of ^{10}Be in rain has remained roughly constant (e.g. at 1.3×10^6 atoms cm^{-2} yr^{-1} per 1000 mm of rain) then as the time-scale and rate of deposition of the Chinese loess have been calculated elsewhere (Maher & Thompson 1992), we can estimate rainfall from eqs (2)–(4). In this second approach to palaeorainfall estimation, high ^{10}Be flux would correspond to high palaeorainfall and low ^{10}Be flux to low palaeorainfall.

If we apply this method to the data of Shen *et al.* (1992) for the interglacial soils S_0 to S_7 at Luochuan, we have from the interglacial intercept in Fig. 5, $C_D = 1.8 \times 10^8$ atom g^{-1} and, from the gradient, an average palaeorainfall of 415 mm yr^{-1}. This average rainfall estimate is much lower than the present-day value ($\approx$650 mm yr^{-1}). The palaeorainfall estimates for the loess horizons L_1 to L_8 are also scattered (Fig. 5). The average rainfall for glacial periods is 210 mm yr^{-1} and the ^{10}Be dust loading 1.6×10^8 atoms g^{-1}. Although the ^{10}Be dust loading intercepts in Fig. 5 are very similar, the considerable scatter about the two regression lines indicates to us that the original ^{10}Be loading of the loess-dust has probably varied over time, and hence that assumption (c) has not held true and that ^{10}Be alone is not a good rainfall indicator.

3.1.3 Method 3: paired magnetic susceptibility/beryllium-10

Heller *et al.* (1993) have used paired magnetic susceptibility/^{10}Be measurements to make quantitative palaeo-

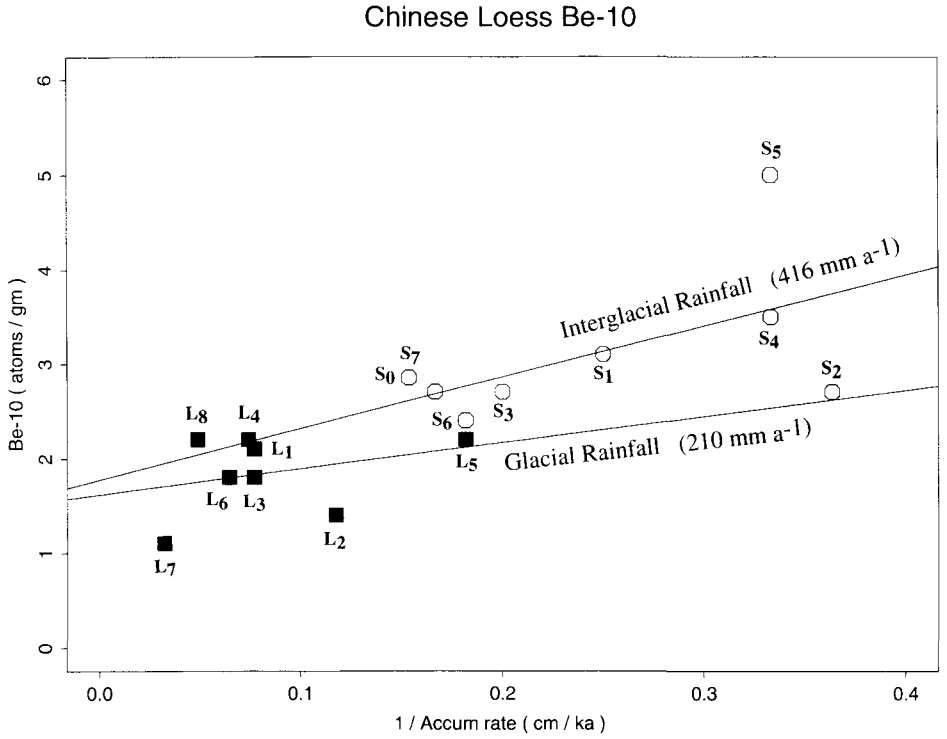

Figure 5. ^{10}Be versus reciprocal accumulation rate at Luochuan. ■, Glacial periods; ○, interglacial. The regression lines (based on Method 2) estimate rainfall on the assumption that the variation in ^{10}Be concentration in Chinese loess depends solely on exposure to rainfall. The Luochuan data, interpreted according to Method 2, reveal higher rainfall during interglacial periods compared with drier glacial periods. However, the absolute differences in ^{10}Be between glacial and interglacial periods are lower than expected. Furthermore, there is considerable scatter about the Method 2 regression lines. Consequently another approach is preferred to explain the ^{10}Be content. We suggest that the primary ^{10}Be loading of the detrital loess particles is a major but variable constituent, which is additional to the site rainfall component. Loess horizons plotting above the regression lines, e.g. S_5, are thus interpreted as having a high primary ^{10}Be dust loading, while loess horizons plotting below the regression lines, e.g. S_2 and L_7, are taken to have had particularly low primary ^{10}Be dust loadings.

rainfall reconstructions. As in Methods 1 and 2, the dust and rainfall contributions have to be separated. By using a combined approach, Heller *et al.* (1993) seek to avoid some of the assumptions inherent in Methods 1 and 2. Nevertheless, certain assumptions still have to be made. Following Beer *et al.* (1993), Heller *et al.* (1993) assume (**e**) that the magnetic susceptibility dust flux (F_D) is proportional to the ^{10}Be dust flux, i.e.

$$F_D = \alpha C_D. \quad (5)$$

They also assume (**f**) that to a first approximation the atmospheric ^{10}Be flux, F_A, remains constant at present-day values (e.g. Brown *et al.* 1989), i.e.

$$F_A = 1.3 \times 10^6 \text{ atoms cm}^{-2} \text{ yr}^{-1}. \quad (6)$$

Under the above assumptions, the ratio of the flux of the *in situ* pedogenic susceptibility (F_X) to the total susceptibility flux (F_S) can be found (Beer *et al.* 1993). Flux F_X is converted to palaeorainfall (Heller *et al.* 1993) using a linear calibration of the pedogenic susceptibility of the S_0 palaeosol against modern rainfall. In essence, in this approach, ^{10}Be is used only to estimate the susceptibility of the original loess-dust.

In general terms, high $\chi/^{10}$Be ratios and high χ flux rates correspond to high palaeorainfall estimates in Method 3. Note that in both Methods 2 and 3, flux calculations based on accumulation rate estimates are needed, in addition to concentration measurements, to reconstruct palaeorainfall.

3.2 Palaeowind indicators

3.2.1 Proxy 1: magnetic susceptibility

Some workers have sought to explain the magnetic susceptibility variations in the loess records in terms of fluctuations in atmospheric circulation in the Northern Hemisphere. Assuming the sedimentation rate of ferrimagnetic minerals to be approximately constant, Kukla *et al.* (1988) suggested a depositional origin for the bulk susceptibility. Kukla & An (1989) suggested that the magnetic susceptibility variations were produced by modulation of wind velocity/frequency and vegetation cover in the source regions, which in turn caused more magnetic material to be supplied in interglacial periods. Others have found this proposal appealing owing to the apparent constancy of magnetic susceptibility influx, which, if real, would be difficult to explain by a non-depositional mechanism. (However, as shown in Table 3, susceptibility flux is not constant in the Loess Plateau.) Many ocean sediment stratigraphers (e.g. Hovan *et al.* 1989; Clemens & Prell 1990) use the constant magnetic susceptibility flux model for the Chinese loess when comparing the loess and marine sequences. While this elegantly derived time-scale is appealing and probably adequate in some contexts, it is not accurate enough to calculate loess flux in detail (e.g. Banerjee 1994).

3.2.2 Proxy 2: particle-size distribution

An *et al.* (1991) and Xiao *et al.* (1995) suggest that the median particle size of the Chinese loess can be regarded as a measure of the strength of winter monsoon winds. In particular, the median particle size of the quartz component is used by Xiao *et al.* (1995) to recognize strong winter monsoonal winds. The quartz component is chosen as the clay fraction may have been significantly increased *in situ* by weathering. Xiao *et al.* (1995) point out that the patterns of variation of median particle size and magnetic susceptibility have many differences, thus supporting the premise that loess susceptibility predominantly reflects pedogenic processes rather than aeolian depositional effects.

3.2.3 Proxy 3: beryllium-10

Shen *et al.* (1992) find a linear relationship between ^{10}Be flux and accumulation rate for 700 ka of deposition at Luochuan. They interpret the relationship to derive a mean ^{10}Be concentration of 2.0×10^8 atoms g^{-1} for the loess-dust at the time of deposition. Beer *et al.* (1993) confirm the linear relationship, finding an average concentration of 2.19×10^8 atoms g^{-1} for the loess-dust, but point out that this average ^{10}Be concentration could be a slight overestimate for the coarser-grained loess-dust of glacial periods.

3.2.4 Proxy 4: rainfall-corrected beryllium-10

In contrast with Shen *et al.* (1992), we suggest that the ^{10}Be concentration of the dust deposited on the Loess Plateau has not remained constant but has shown substantial variation both within and between glacial and interglacial periods. Because of the great affinity of ^{10}Be for clay surfaces, any changes in the particle size distribution of the finest dust blown onto a site is a powerful means of producing variable ^{10}Be loading. In our scenario, ^{10}Be variations, once corrected for the post-depositional ^{10}Be rainfall flux (Table 4), are a potential indicator of changing dust sources. We find a low ^{10}Be loading for loess L_2, which, at Baoji, is an unusually clay-poor loess (Rutter 1992) but also for L_7 which is not particularly fine grained. We estimate a high loess ^{10}Be loading in L_4, which is relatively clay-rich loess (Rutter 1992). In the palaeosols, we find the highest ^{10}Be loading in palaeosol S_5, which is notably clay-rich (Rutter 1992) and a low ^{10}Be loading for S_2.

3.3 A unified particle-size/susceptibility/^{10}Be palaeoclimatic model

Particle size, magnetic susceptibility and ^{10}Be clearly covary in the Chinese loess, and all have been responsive to climatic change. We interpret the changes in the three parameters as predominantly reflecting past changes in palaeowind and/or palaeorainfall. At Luochuan, the detailed magnetic and ^{10}Be measurements (Table 5) can be compared and the relative importance of wind and rain estimated. In our model, we first use magnetic susceptibility to estimate palaeorainfall following Method 1. Next, ^{10}Be is corrected for a palaeorainfall contribution using eqs (2)–(4), and the original ^{10}Be dust loadings are estimated. Particle-size variation and the calculated primary ^{10}Be loadings are used as a measure of changing wind intensity and source materials.

From our unified model we find that:

(1) The major variations in the particle size distribution of Chinese loess relate to source variations and monsoonal wind strength.

(2) The magnetic susceptibility of the original loess-dust is presumed to be weak (typically 20×10^{-8} m^3 kg^{-1}) and to have varied little in space and time.

(3) Variations in source material and clay content of the primary loess-dust give rise to very variable primary ^{10}Be

Table 5. Luochuan susceptibility and ^{10}Be data at selected loess–palaeosol horizons.

Stratigraphy				Data			Age Model			Assumed	Calculated	
Unit	^{18}O Stage	Depth Top m	Depth Base m	Density g m^{-3}	^{10}Be 10^8atg^{-1}	χ $10^{-8}m^3kg^{-1}$	Duration ka	ka	Acc^n rate cm ka^{-1}	χ dust $10^{-8}m^3kg^{-1}$	Rainfall* mm a^{-1}	$^{10}Be_{dust}$+ 10^8at g^{-1}
		Z		σ	C_B	χ_B	t		$\delta Z/\delta t$	χ_D	C_D	
S_0	1	0.0	1.3	1.3	2.7	200	0	11	15	20	670	2.0
LL_1	2	1.3	3.5	1.0	1.5	45	11	25	16	20	500	1.0
S_1	5	9.7	11.7	1.3	3.5	260	70	128	4.4	20	695	1.0
L_2	6	11.7	17.6	1.0	1.2	30	128	186	10	20	420	0.5
L_5	12	30.0	35.6	1.0	1.9	30	426	476	11	20	420	1.3
S_5	13	35.6	40.2	1.3	6.5	280	476	530	11	20	700	5.5
L_7	18	46.9	47.9	1.0	1.2	40	696	703	14	20	480	0.7
L_9	22	54.5	58.5	1.0	0.8	20	788	810	18	20	220	0.6

* Calculation based on equation 1
\+ Calculation based on equations 2 to 4

loadings. The initial ^{10}Be concentrations are found to have ranged from 0.5×10^8 to 5.5×10^8 atoms g^{-1}.

(4) Chinese loess is assumed to have an almost perfect ^{10}Be retention capacity. Changes in rainfall lead to significant but variable post-depositional increases in ^{10}Be concentration of between 0.2×10^8 and 2.5×10^8 atoms g^{-1}. Post-depositional increases in clay content have little effect on the ^{10}Be concentration, as the number of adsorption sites is not a limiting factor; however, *in situ* increases in clay content may have caused some redistribution of the ^{10}Be between size fractions in the loess.

(5) A good match is found between clay content and primary ^{10}Be loading. The extremely high primary ^{10}Be loadings found for some loess/palaeosol units indicate dust transport from a source area which has undergone prolonged weathering in a high-rainfall area, rather than rapid erosion in a desert environment.

(6) Pedogenic processes are taken to have caused only minor modification of the loess particle size since deposition, e.g. post-depositional increases in clay content, as in many soils, are assumed to have been slow and long-term (Fig. 6).

(7) In contrast, pedogenic processes, controlled by the annual rainfall, are assumed to have dominated the growth of bulk susceptibility in the loess through the rapid neoformation of strong ferrimagnets.

We reiterate that in our model magnetic susceptibility variations in the Chinese loess/soil sequences are almost exclusively produced by palaeorainfall variations which have controlled the weathering and mineralogy of iron oxides. The particle-size variations are taken predominantly to reflect changing palaeowind velocity, with only rather minor modification to particle size by post-depositional weathering processes. Finally, the ^{10}Be variations in the loess are explained by a more complex palaeoclimatic origin: we ascribe roughly equal, but varying, importance to a post-depositional ^{10}Be palaeorainfall component and to an original ^{10}Be dust-loading component and little, if any, dependence on post-depositional weathering.

4 DISCUSSION

Trace element (Zhang *et al.* 1993, 1994) and isotopic analyses (Nakai, Halliday & Rea 1993) indicate a source region for the loess-dust from desert and local sources to the north and north-west (Fig. 1a). These source areas are noticeably drier than the Loess Plateau (Fig. 1b). To account for the level of ^{10}Be loading, much of the Quaternary dust must have spent one million years or more in a wet environment adsorbing ^{10}Be, before arriving on the Loess Plateau. We speculate that the dust originally weathered further to the west, e.g. on the Tibetan plateau or its margins, before moving to the desert and then to the Chinese Plateau.

Eyre (1994) and Eyre & Shaw (1994) suggest that an important magnetic constituent of the Chinese loess is a superparamagnetic maghemite. Eyre (1994) further suggests an origin for these magnetic minerals in the nearby desert regions and transportation to the Chinese Loess Plateau at a steady rate as envisaged by Kukla *et al.* (1988) and by Kukla & An (1989). However, the accumulation rate calculations summarized in Table 3 show that this process cannot explain the magnetic concentration fluctuations whereas *in situ* pedogenic enhancement (Le Borgne 1955) clearly can. Such *in situ* enhancement processes are ideal for generating superparamagnetic ferrimagnets of the properties described by Eyre & Shaw (1994). Furthermore, dry oxidizing climates of desert areas are more likely to hinder the production of ferrimagnetic minerals than to accelerate it.

Given that *in situ* magnetic enhancement during soil development accounts for the main variations in susceptibility, it is possible to use magnetic susceptibility alone as a palaeorainfall indicator, *if* magnetic enhancement takes place rapidly. Fig. 6 summarizes some data on soil development. It shows the great contrast in development rates that are to be found. Some processes are slow while others are relatively rapid. Noticeably organic carbon increases rapidly and our assumption is that magnetic susceptibility is partly controlled by organic content.

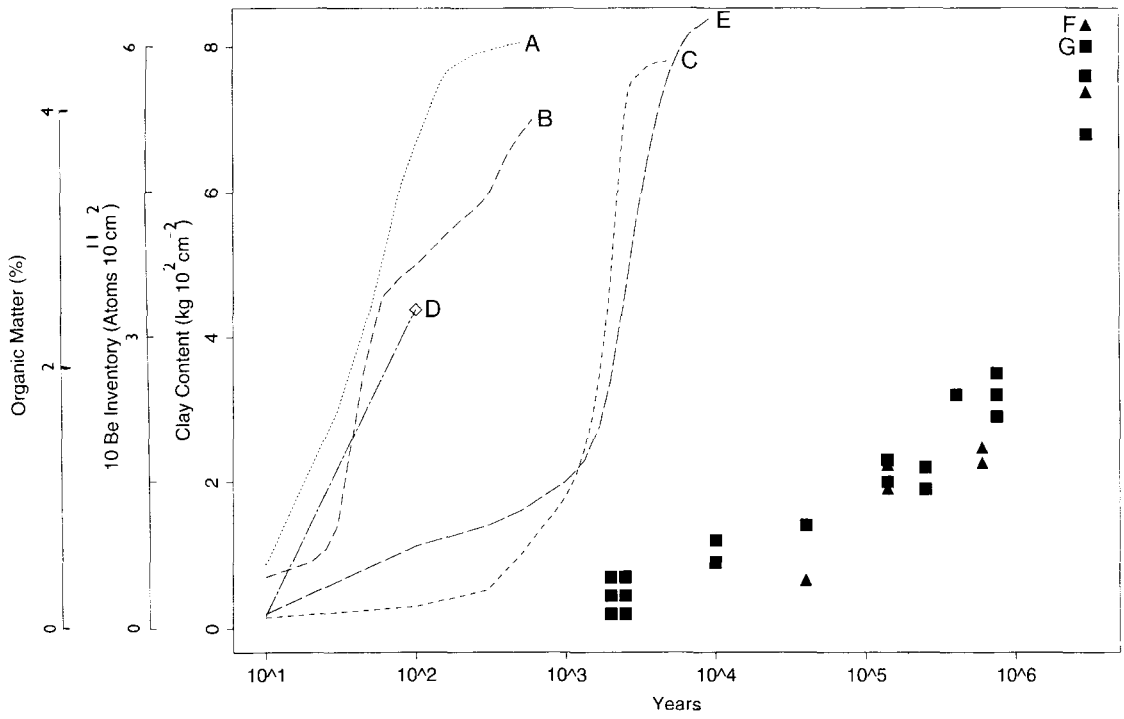

Figure 6. Chronofunctions for: (1) organic matter (%) build up: (A) Stork (1963), (B) Dickson & Crocker (1953), (C) Mahaney (1970), (D) Hallberg, Wollenhaupt & Miller (1978); (2) organic carbon (kg m^{-2}): (E) Seyers, Adams & Walker (1970); (3) ^{10}Be influx (atoms 10^{11} cm^{-2}: (▲) Pavich *et al.* (1986); (4) clay accumulation (kg 10^2 cm^{-2}): (■) Pavich *et al.* (1986). Note how organic matter concentration increases rapidly in the first few decades or centuries of soil formation and then stabilizes. Clay and ^{10}Be content in contrast build up gradually over a million years of rainfall and weathering. An essential assumption in our Method 3 of palaeorainfall reconstruction is that susceptibility in the Chinese loess soils builds up rapidly to approach a steady state in a few thousand years or less.

We suggest that the competing processes of iron reduction and oxidation determine the degree of magnetic enhancement. Iron in ionic (Fe^{3+}) form is released into the overlying soil by weathering of primary iron-bearing minerals. The Fe^{3+} ions released may be either incorporated *in situ* into an iron oxide form, or reduced and mobilized by the soil solution before subsequent re-oxidation and precipitation elsewhere in the soil profile. In humid temperate areas, the most prevalent pedogenic iron oxide is goethite; in drier, more oxic regimes, haematite is dominant. To produce the ferrimagnetic mineral, magnetite, from these weakly magnetic iron oxides, some reduction of Fe^{3+} to Fe^{2+} is required. Organic content and temporary, rainfall-induced wetness generate iron-reducing conditions in the soil through biological activity (Lovley *et al.* 1987), which in turn promotes the efficient chemical precipitation of ferrimagnetic iron oxides. Enhancement may also occur by strictly inorganic means, such as the process of induced hydrolysis (Tamaura, Ito & Katsora 1983). Both bacterial activity and chemical precipitation of magnetite appear favoured by near-neutral pH conditions (Lovley *et al.* 1987; Taylor, Maher & Self 1987). Conversely, oxidation during dry periods or over extended periods of time causes the pedogenic magnetite to convert via surface oxidation to maghemite or, more completely (via dissolution and reprecipitation), to the less magnetic minerals, haematite and goethite. The dynamic balance between the two ongoing processes of iron reduction and oxidation determines the level of magnetic enhancement. For the Chinese loess soils, our contention is that iron reduction, as modulated by rainfall, is the limiting process.

5 CONCLUSIONS

(1) A range of dating techniques (magnetostratigraphy; uranium series; radiocarbon; thermoluminescence and matching of susceptibility (or ^{10}Be) to the $\delta^{18}O$ deep-sea isotopic record) provide a broadly concordant stratigraphy for the Chinese loess.

(2) Despite the broad agreement of the above six dating techniques, accumulation rates remain poorly constrained.

(3) The Chinese loess contains a detailed terrestrial proxy record of past climates.

(4) Particle-size variations reflect changes in the palaeowinds of the Siberian high-pressure system.

(5) Detrital particle size, in particular clay content, is an important control on the ^{10}Be concentration.

(6) Primary ^{10}Be loading of the detrital particles must have been high, with this source material exposed to high rainfall for upwards of one million years before transportation and deposition on the Chinese Loess Plateau.

(7) All accumulation rates and fluxes have varied both spatially and temporally and cannot be assumed to have remained constant.

(8) Magnetic susceptibility variations reflect palaeorainfall at the deposition site, high susceptibility corresponding to high palaeorainfall.

ACKNOWLEDGMENTS

We are grateful to Julii Brainard who provided the GIS data in Fig. 1 and to the Lamont Doherty Geology core store staff

for supplying Pacific sediments for susceptibility measurement. Part of this work was funded by a NERC (UK) research grant to BAM. The TL datings were carried out by L. P. Zhou as part of the NERC (UK) research project.

REFERENCES

An, Z.S., Kukla, G.J., Porter, S.J. & Xiao, J., 1991. Magnetic susceptibility evidence of monsoon variations on the Loess Plateau of central China during the last 130,000 years, *Quat. Res.,* 36, 29-36.

Banerjee, S.K., 1994. Contributions of fine particle magnetism to reading the global paleoclimate record, *J. appl. Phys.,* **75(1),** 5925-5930.

Beer, J., Shen, C, Heller, F., Liu, T., Bonani, G., Dittrich, B., Suter, M. & Kubik, P.W., 1993. ^{10}Be and magnetic susceptibility in Chinese loess, *Geophys. Res. Lett.,* **20(1),** 57-60.

Brown, L., Stensland, G.J., Klein, J. & Middleton, R., 1989. Atmospheric deposition of ^{7}Be and ^{10}Be, *Geochim. cosmochim. Ada,* **53,** 135-142.

Clemens, S.C. & Prell, W.L. 1990. Late Pleistocene variability of Arabian Sea summer monsoon winds and continental aridity: eolian records from the Kthogenic component of deep-sea sediments, *Palaeoceanography,* 5, 109-145.

Dickson, A.B. & Crocker, R.L., 1953. A chronosequence of soils and vegetation near Mt Shasta, California. II The development of forest floors and the carbon and nitrogen profiles of the soils, J. *Soil Sci.,* 4, 142-154.

Eyre, J.K., 1994. Magnetic mineralogy of Chinese loess, *PhD thesis,* University of Liverpool.

Eyre, J.K. & Shaw, J., 1994. Magnetic enhancement of Chinese loess—the role of yFe_2O_3?, *Geophys. J. Int.,* **117,** 265-271.

Hallberg, G.R., Wollenhaupt, N.C. & Miller, G.A., 1978. A century of soil development in spoil derived from loess in Iowa, *Soil Sci. Soc. Am. J.,* 42, 339-343.

Heller, F. & Liu, T., 1982. Magnetostratigraphical dating of loess deposits in China, *Nature,* **300,** 431-433.

Heller, F. & Liu, T., 1986. Magnetism of Chinese loess deposits, *J. Geophys. Res.,* **77,** 125-141.

Heller, F., Shen, CD., Beer, J., Liu, X.M., Bronger, A., Suter, M. & Bonani, G., 1993. Quantitative estimates of pedogenic ferromagnetic mineral formation in Chinese loess and palaeoclimatic implications/ *Earth planet. Sci. Lett.,* 114,385-390.

Hovan, S.A., Rea, D.K., Pisias, N.G. & Shackleton, N.J., 1989. A direct link between the China loess and marine <5^{18}O records: aeolian flux to the north Pacific, *Nature,* **340,** 296-298.

Kukla, G. & An, Z., 1989. Loess stratigraphy in central China, *Palaeogeog. Palaeoclimat. Palaeoecol,* **72,** 203-225.

Kukla, G., Heller, F, Liu, X.M., Xu, T.C., Liu, T.S. & An, Z.S., 1988, Pleistocene climates in China dated by magnetic susceptibility, *Geology,* 16, 811-814.

Le Borgne, E., 1955. Susceptibility magnetiqueanprmale/du sol superficiel, *Ann. Geophys.,* 11, 399-419.

Lovley, D.R., Stolz, J., Nord, G.L. & Phillips, E.J.P., 1987. Anaerobic production of magnetite by a 'dissimilatory iron-reducing microorganism, *Nature,* **330,** 252.

Mahaney, W.C., 1970. Soil genesis on deposits of fteoglacial'and lafe Pleistocene age in the Indian Peaks of the Colorado Front Range, *PhD thesis,* University of Colorado.

Maher, B.A. & Thompson, R., 1992. Paleoclimatic significance of the mineral magnetic record of the Chinese loess and paleosols, *Quat. Res.,* **37,** 155-170.

Maher, B.A., Thompson, R. & Zhou, L.P., 1994. Spatial and temporal reconstructions of changes in the Asian palaeomonsoon: a new mineral magnetic approach, *Earth planet. Sci. Lett.,* **125,** 461-471.

Nakai, S., Halliday, A.N. & Rea, D.K., 1993. Provenance of dust in the Pacific Ocean, *Earth planet. Sci. Lett.,* **119,** 143-157.

Pavich, M.J., Brown, L., Harden, J., Klein, J. & Middleton, R., 1986. ^{10}Be distribution in soils from Merced river terraces, California, *Geochim. cosmochim. Acta,* **50,** 1727—1735.

Rendell, H. & Townsend, P.D., 1988. Thermoluminescence dating of a 10M loess profile in Pakistan, *Quat. Sci. Rev.,* 7, 251-255.

Rutter, N., 1992. Presidential Address, XIII INQUA Congress 1991: Chinese loess and global change, *Quat. Sci. Rev.,* 11, 275-281.

Seyers, J.K., Adams, J.A. & Walker, T.W., 1970. Accumulation of organic matter in a chronosequence of soils on wind-blown sand in New Zealand, *J. Soil Sci.,* 21, 146-153.

Shen, C, Beer, j., Liu, T.S., Oeschger, H., Bonani, G., Suter, M. & Wolfli, W., 1992. ^{10}Be in Chinese loess, *Earth planet. Sci. Lett.,* **109,** 169-177.

Stork, A., 1963. Plant immigration in front of retreating glaciers, with examples from the Kebnekajse area, N. Sweden, *Geogr. Ann.,* **XLV,** 1-22.

Tamaura, Y., Ito, K. & Katsura, T., 1983. Transformation of aFeO(OH) to Fe_3O_4 by adsorption of iron (II) ion on aFeO(OH), *J. Chem. Soc. Dalton Trans.,* 1, 189-194.

Taylor, R.M., Maher, B.A. & Self, P.G., 1987. Magnetite in soils: I. The synthesis of single domain and superparamagnetic magnetite, *Clay Miner.,* **22,** 411-422.

Thompson, R. & Clark, R.M., 1993. Quantitative marine sediment core matching using a modified sequence-slotting algorithm, in *High Resolution Stratigraphy,* pp. 39-49, eds Hailwood, E.A. & Kidd, R.B., The Geological Society of London Special Publication No. 70, London.

Wintle, A.G., 1990. A review of current research on TL dating of loess, *Quat. Sci. Rev.,* 9, 385-397.

Xiao, J., An, Z., Kumai, H., Yoshikawa, S. & Porter, S.C, 1995. Grain size of quartz as an indicator of winter monsoon strength on the Loess Plateau of central China during the last 130,000 years, *Quat.* Res., 43, 22-29.

Zhang, X., Arimoto, R., An, Z., Chen, T., Zhang, G., Zhu, G. & Wang, X., 1993. Atmospheric trace elements over source regions for Chinese dust: concentrations, sources and atmospheric deposition on the Loess Plateau, *Atmos. Env., 21 A,* 2051-2067.

Zhang, X., An, Z., Chen, T., Zhang, G., Arimoto, R. & Ray, B.J., 1994. Late Quaternary records of the atmospheric input of eolian dust to the centre of the Chinese Loess Plateau, *Quat. Res.,* 41, 35-43.

Zheng, H.B., An., Z.S. & Shaw, J., 1992. New contributions to Chinese Plio-Pleistocene magnetostratigraphy, *Phys. Earth planet. Inter., fb,* 146-153.

Zhou, W., Aii., Z., Lin, B., Xiao, J., Zhang, J., Xie, J., Zhou, M., Porter, S.C, Head, M.J. & Donahue, D.J., 1992. Chronology of the Baxie loess profile and the history of monsoon climates in China between 17,000 and 6000 years BP, *Radiocarbon,* 34, 818-825.

Zhu, R.X, Zhou, L.P., Laj, C, Mazaud, A. & Ding, Z.L., 1994. The Blake geomagnetic polarity episode recorded in Chinese loess. *Geophys. Res. Lett,* 21(8), 697-700.